https://doi.org/10.48048/tis.2025.9586

Synthesis and Bioinformatics Study of 2-Nitrocinnamaldehyde Derivatives as an Anti MCF-7 Breast Cancer Cells

Alidya Fitri Kusuma Wardani[1], Muhammad Naufal[2], Madyawati Latief[1], Indra Lasmana Tarigan[1], Juliandri Juliandri[2] and Jamaludin Al-Anshori[2,*]

[1]Departement of Chemistry, Faculty of Science and Technology, Jambi University, Jambi 36361, Indonesia
[2]Departement of Chemistry, Faculty of Mathematics and Natural Sciences, Universitas Padjadjaran, Jawa Barat 45363, Indonesia

([*]Corresponding author's e-mail: jamaludin.al.anshori@unpad.ac.id)

Received: 22 December 2024, Revised: 23 January 2025, Accepted: 30 January 2025, Published: 20 March 2025

Abstract

Conventional and systemic treatments of breast cancer are commonly found to expose unexpected side effects. Thus, a new drug design is intensively explored to anticipate the related risks. This work aimed to synthesize and characterize the chalcone derivatives based on a cinnamaldehyde skeleton (**9** - **12**). Further biological assay of the derivatives against MCF-7 breast cancer cell lines and their molecular docking analysis was also performed to obtain a more potential chemical structure for the active compounds. Four compounds of a 2-Nitrocinnamaldehyde-based scaffold, 1-(4-aminophenyl)-5-(2-nitrophenyl)-penta-2,4-dien-1-one (**9**), 1-(4-bromophenyl)-5-(2-nitrophenyl)-penta-2,4-dien-1-one (**10**), 5-(2-nitrophenyl)-1-(p-tolyl)-penta-2,4-dien-1-one (**11**), and 5-(2-nitrophenyl)-1-(pyridine-3-yl)-penta-2,4-dien-1-one (**12**) were successfully synthesized with a chemical yield of 29 - 99 %. The synthetic method employed a one-pot Claisen-Schmidt coupling reaction using a NaOH/KOH base catalyst, while their characterization was based on spectroscopic data and literature comparison. An *in-vitro* MTT bioassay against MCF-7 cancer cells revealed the IC_{50} values of the derivatives of **9**, **10**, **11**, and **12** were 178, 376, >500, and 118.20 µg/mL, respectively. Molecular docking showed that the most potent compound in this series (**12**) had the lowest binding energy (–8.56 kcal/mol) and created an essential H-bond with hinge region residue, Met793. Docking-based structural optimization of **12** showed that incorporating 3 important pharmacophores commonly found in EGFR kinase inhibitors, fused heterocyclic, hydrophobic group, and propylmorpholine moiety, resulted in lower binding energy (–9.41 kcal/mol). Perhaps the modified **12** could exhibit a more potent toxicity against MCF-7.

Keywords: Anticancer, Bioinformatics, Cinnamaldehyde, Claisen-Schmidt, Docking, *In-vitro* assay, MCF-7

Introduction

Breast cancer is the 2nd most common cancer that causes death after lung cancer, suffered 100 times more by women than men [1]. Conventional treatment options for breast cancer include local treatments such as surgery and radiation therapy, which treat the tumor without affecting the rest of the body, and systemic treatments such as chemotherapy, endocrine therapy, targeted therapy, and immunotherapy, which virtually reach cancer cells anywhere [2]. In particular, chemotherapy is known to be effective in treating various types of cancer; [3] however, inadequate incidence of resistance, strong side effects, and efficacy are reported [4] and ultimately lead to death [5]. Therefore, new drug designs are needed to minimize the risk of unexpected side effects by developing active compounds or drugs through structure modification based on known or potent anti-cancer agents. The structural modification can be done by synthesis, in which the analogs will have pharmacological properties similar to the parent compound or even better pharmacological activity [6-9].

Since the chalcone scaffold was often discovered in the template of medicinal chemistry for natural or synthetic drugs [9,10], it inspired further synthetic modification based on SAR to find more bioactive compounds. Chalcone derivatives generally demonstrated various bioactivities such as antiproliferative, antifungal, antibacterial, antiviral, antimalarial, anticancer, and antioxidant [10]. Further hybridization with a heterocyclic moiety appeared as promising future drug candidates with similar or superior activity compared to the standard [11]. The most classical and published synthetic method of chalcone employs Claisen-Schmidt condensation [12], which is a simple experimentally and highly efficient C-C coupling with less restriction to the complexity of the target molecules [10]. Further modification of the chalcone structure with an unsaturated α,β-ketone compound, 2 aromatic rings (A and B), and 1 unsaturated α,β carbon atom demonstrated increasing bioactivities. For instance, when the A ring contains ethyl, methyl, or alkyl groups, the B ring contains hydrophobic groups such as halogens, nitro, and cyano, as well as the double bond moiety [13].

According to Wang *et al*. [14], chalcone-naphthalene substituted 3-hydroxy-4-methoxyphenyl (**1**) and 3-amino-4-methoxyphenyl (**2**) derivatives have the best toxicity against MCF-7 cells with IC_{50} respectively 1.42 ± 0.15 and 2.75 ± 0.26 µM. Another chalcone compound containing mono methoxy substituent at the aromatic ring (**3**) has been reported to have anticancer activity against MCF-7 cells with an IC_{50} value of 19.15 µg/mL [15]. Based on research reported by Mai *et al*. [16], the methoxy-substituted chalcone compound (**4**) was also reported to be cytotoxic to MCF-7 cells with an IC_{50} value of 63.90 µg/mL. In addition, chalcone with a trimethoxyphenyl group (**5**) was successfully synthesized and exhibited a cytotoxic effect with IC_{50} 0.21 µM [17]. Further development of the chalcone derivatives inspired by an anti-cancer leinamycin was also performed by Weldon *et al*. [18] to result in cinnamylideneacetophenones derivatives with aryl substitutions employing modified Claisen-Schmidt condensation reaction. Potent cytotoxicity against MCF-7 breast cancer cells was exposed by the derivatives **6** 1-(furan-2-yl)-5-(2-nitrophenyl)penta-2,4-dien-1-one) and **7** 5-(2-nitrophenyl)-1-phenylpenta-2,4-dien-1-one) bearing a 2-nitro group on the B ring with sub-micromolar cytotoxicity (IC_{50} = 71 and 1.9 nM) (**Figure 1**).

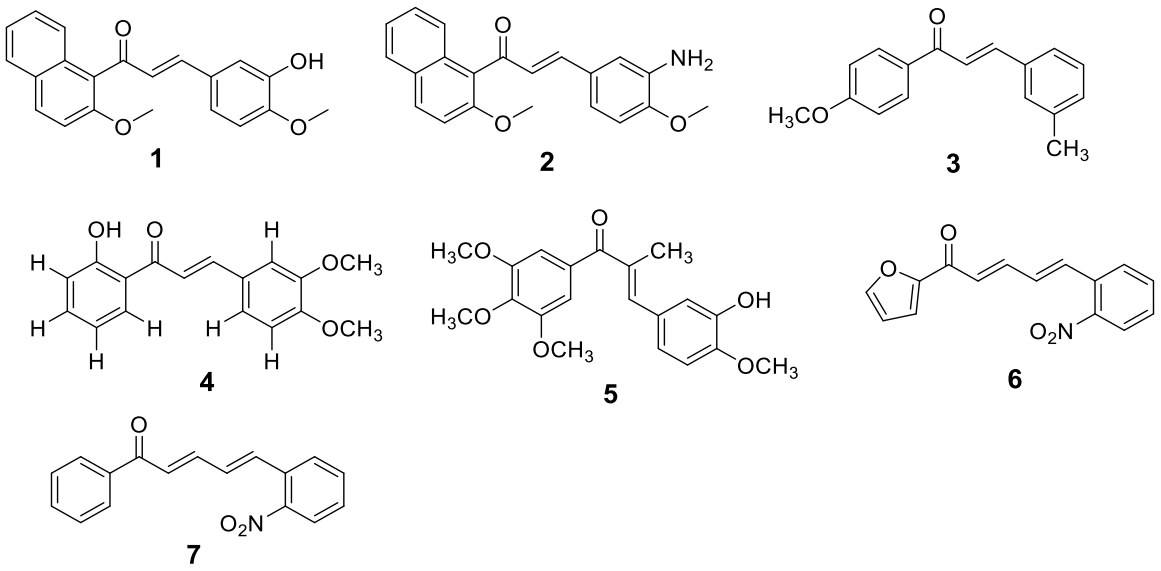

Figure 1 Various anticancer-based chalcone derivatives against MCF-7 breast cancer cells.

In this work, we synthesized and characterized 4 compounds based on the cinnamaldehyde skeleton (**9** - **12**). Further biological assay was also conducted on the derivatives against MCF-7 breast cancer cell lines. To the best of our data screening on the SciFinder-ACS and Reaxys-Elsevier, the 2 derivatives (**9** and **12**) were new

compounds, and none of any literature reported the related bioassay of all derivatives. Further analysis of their interaction mechanism employing a bioinformatic approach was also achieved to modify the chemical structure exhibiting more potential cytotoxicity computationally.

Materials and methods

Materials

Pro analyst and synthetic grade chemicals were purchased from Sigma-Aldrich Company. All solvents were used without further purification. Thin-layer chromatography was performed on silica gel GF_{254}. The uncorrected melting points were measured on a Mettler Toledo digital melting point apparatus. The molar absorptivity was determined using an Agilent UV/Vis spectrophotometer, while the infra-red spectra were obtained on Perkin Elmer FTIR with potassium bromide (KBr) pellets. Exact masses were obtained using a high-resolution mass spectrometer (Waters Xevo QTOF HR-MS Lockspray). ^{1}H and ^{13}C NMR spectra were recorded on Agilent 500 MHz and 125 MHz spectrometers in $CDCl_3$ or DMSO-d_6 and referenced relative to the solvent peaks.

Synthetic procedure

The analog synthetic procedure referred to the method reported by Weldon *et al*. [18] with some modifications (Scheme 1).

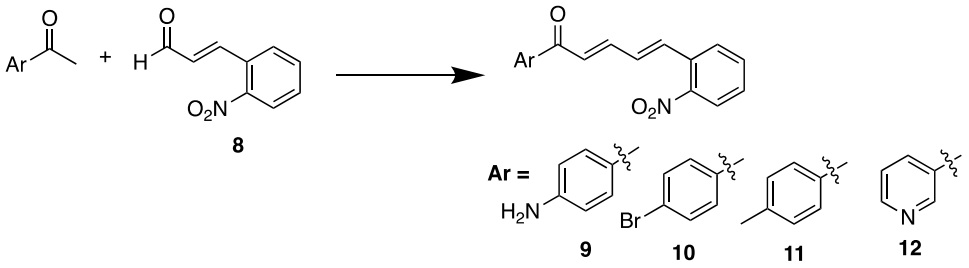

Scheme 1 Reagents and conditions: (**9**) NaOH/EtOH, rt, 6 h; (**10** and **11**) KOH/MeOH:H_2O, 50 °C 1 h; (**12**) KOH/MeOH:H_2O, rt, 30 min.

Synthesis of 1-(4-aminophenyl)-5-(2-nitrophenyl)-penta-2,4-dien-1-one (9)

4-Aminoacetophenone (0.10 g, 0.73 mmol, 1 eq) was dissolved into a round bottom flask with 5 mL of ethanol while stirring. Later, 0.74 mL of 40 % NaOH (*b*/*v*) was added, stirring the mixture for 2 min. Finally, 2-nitrocinnamaldehyde (0.13 g, 0.73 mmol, 1 eq) was added to the mixture and further stirred at room temperature for 6 h. Furthermore, the reaction mixture was diluted with cold distilled water and neutralized using 10 % HCl. The precipitated solid was then filtered and washed with distilled water. Upon purification on a silica gel column chromatography eluted by *n*-hexane:ethylacetate (2:1, *v*/*v*), a yellowish solid was obtained with a chemical yield of 29 % (0.063 g). Melting point (172.1 - 172.4 °C) IR (KBr, cm^{-1}) 3341 (strong, -NH_2), 1728 (strong, C=O), 3048 (medium, C-H aromatic), 1543 (strong, -NO_2) and 1573 (C=C aromatic). UV-Vis absorbance spectra in methanol (c = 1×10^{-5} M), λ_{max}/nm (ε/M^{-1} cm^{-1}); 271 (60073), 376 (36606). ^{1}H-NMR (500 MHz, DMSO) δH/ppm: 8.00 (d, J = 7.8 Hz, 1H), 7.91 (d, J = 7.3 Hz, 1H), 7.78 (m, 3H), 7.60 - 7.56 (m, 1H), 7.44 (t, 2H), 7.38 - 7.32 (m, 1H), 7.27 - 7.21 (m,1H), 6.61 (d, J = 8.2 Hz, 2H), 6.18 (s, 2H). ^{13}C-NMR (125 MHz, DMSO) δC/ppm: 186.14, 154.34, 148.36, 141.10, 133.89, 133.68, 132.61, 131.31, 131.27, 131.18, 129.89, 128.68, 128.48, 125.51, 124.95, 113.17, 113.12. ToF-HRMS (ES^+) m/z: $[M + H]^+$ calculated for $C_{17}H_{14}N_2O_3$ 295.1083; found 295.1084.

Synthesis of 1-(4-bromophenyl)-5-(2-nitrophenyl)-penta-2,4-dien-1-one (10)

3-Bromoacetophenone (0.03 g, 0.18 mmol, 1 eq) was placed into a round bottom flask and then dissolved with 10 mL MeOH:H_2O (1:1). Subsequently, 2-nitrocinnamaldehyde (0.10 g, 0.56 mmol, 3 eq) and KOH (0.11 g, 1.88 mmol, 10 eq) were added into the mixture while being stirred at room temperature followed by reflux at 50 °C for 1 h. The reaction mixture was then neutralized with 10 % HCl (pH 7), filtered, and

finally washed with ethanol to yield a brownish solid (86 %, 0.058 g). Melting point (168.5 - 168.7 °C). IR (KBr, cm^{-1}) 3105 (medium, C-H aromatic), 1663 (strong, C=O), 1514 (strong, -NO_2) and 1567 (medium, C=C aromatic). UV-Vis absorbance spectra in methanol (c = 2×10^{-5} M), λ_{max}/nm (ε/M^{-1} cm^{-1}); 323 (18645). ^{1}H-NMR (500 MHz, $CDCl_3$) δH/ppm: 8.00 (d, J = 8.7 Hz, 1H), 7.83 (d, J = 8.5 Hz, 2H), 7.71 (d, J = 7.7 Hz, 1H), 7.63 (t, 3H), 7.60 - 7.56 (m, 1H), 7.53 (s, 1H), 7.48 (m, 1H), 7.08 (d, J = 15.0 Hz, 1H), 6.96 (dd, J = 15.3, 11.1 Hz, 1H). ^{13}C-NMR (125 MHz, $CDCl_3$) δC/ppm: 189.23, 148.08, 144.07, 136.58, 136.24, 133.20, 131.97, 131.60, 131.39, 129.95, 129.90, 129.37, 128.32, 128.31, 128.03, 127.06, 124.98. ToF-HRMS (ES^+) m/z: $[M + H]^+$ calculated for $C_{17}H_{12}BrNO_3$ 358.0079; found 358.0104.

Synthesis of 5-(2-nitrophenyl)-1-(p-tolyl)-penta-2,4-dien-1-one (11)

3-Methylacetophenone (0.02 g, 0.18 mmol, 1 eq) was placed into a round bottom flask and then dissolved with 10 mL MeOH:H_2O (1:1). Afterward, 2-nitrocinnamaldehyde (0.10 g, 0.56 mmol, 3 eq) and KOH (0.04 g, 0.75 mmol, 4 eq) were added into the mixture while being stirred at room temperature for a while. The reaction was further refluxed at 50 °C for 1 h. The precipitated product was then filtered and washed with a small amount of ethanol to produce a brownish solid with a 77 % (0.043 g) chemical yield. Melting point (120.4 - 121.8 °C). IR (KBr, cm^{-1}) 3043 (moderate, C-H aromatic), 1735 (strong, C=O), 1446 (moderate, -CH methyl), 1520 (strong, -NO_2) and 1569 (middle, C=C aromatic). UV-Vis absorbance spectra in methanol (c = 1×10^{-5} M), λ_{max}/nm (ε/M^{-1} cm^{-1}); 316 (31253). ^{1}H-NMR (500 MHz, CDC_{l3}) δH/ppm: 7.99 (d, J = 8.2 Hz, 1H), 7.88 (d, J = 8.1 Hz, 2H), 7.72 (d, J = 7.8 Hz, 1H), 7.64 - 7.55 (m, 2H), 7.50 - 7.45 (m, 2H), 7.30 (d, J = 8.0 Hz, 2H), 7.14 (d, J = 15.1 Hz, 1H), 6.97 (dd, J = 15.3, 11.1 Hz, 1H), 2.43 (s, 3H). ^{13}C-NMR (125 MHz, $CDCl_3$) δC/ppm: 190.29, 148.48, 144.17, 143.54, 135.82, 135.80, 135.73, 133.56, 132.17, 132.14, 129.77, 129.59, 129.02, 128.98, 128.71, 128.25, 125.35, 22.09. ToF-HRMS (ES^+) m/z: $[M + H]^+$ calculated for $C_{18}H_{15}NO_3$ 294.1130; found 294.1193.

Synthesis of 5-(2-nitrophenyl)-1-(pyridine-3-yl)-penta-2,4-dien-1-one (12)

3-Acetylpyridine (0.02 g, 0.18 mmol, 1 eq) was transferred into a round bottom flask and dissolved with 10 mL MeOH:H_2O (1:1). 2-Nitrocinnamaldehyde (0.1 g, 0.564 mmol, 3 eq) and KOH (0.03 g, 0.56 mmol, 3 eq) were then mixed while being stirred for 30 min at room temperature. A 99 % (0.052 g) yield of yellowish-green solid was obtained upon filtration and washing the precipitation with ethanol. Melting point (181.7 - 182.1 °C). IR (KBr, cm^{-1}) 3065 (medium, C-H aromatic), 1661 (strong, C=O), 1518 (strong, -NO_2) and 1567 (medium, C=C aromatic). UV-Vis absorbance spectra in methanol (c = 1×10^{-5} M), λ_{max} (ε/M^{-1} cm^{-1}); 325 (51064). ^{1}H-NMR (500 MHz, $CDCl_3$) δH/ppm: 9.17 (s, 1H), 8.80 (m, 1H), 8.25 (d, J = 7.9 Hz, 1H), 8.00 (d, J = 8.2 Hz, 1H), 7.73 (d, J = 7.7 Hz, 1H), 7.63 (m, 2H), 7.55 (m, 1H), 7.50 (d, 1H), 7.46 (m, 1H), 7.11 (d, J = 15.1 Hz, 1H), 6.99 (dd, J = 15.3, 11.1 Hz, 1H). ^{13}C-NMR (125 MHz, $CDCl_3$) δC/ppm: 189.56, 153.92, 150.33, 148.75, 145.29, 137.53, 136.52, 133.92, 133.86, 132.16, 131.86, 130.16, 129.04, 127.46, 125.67, 124.38. ToF-HRMS (ES^+) m/z: $[M + H]^+$ calculated for $C_{16}H_{12}N_2O_3$ 281.0926; found 281.0924.

MTT cytotoxic assay

The bioassay method referred to the one reported by Zainuddin *et al.* [19] and Mayanti *et al*. [20]. Firstly, the MCF-7 cells at 3×10^4 cells cm^{-3} density were cultivated in 96-well, followed by incubation at 37 °C under a 5 % CO_2 atmosphere for 24 h to attach and grow the cell. Afterward, the stock solution samples were prepared in DMSO, diluted into various desirable concentrations with PBS buffer, and added to the well plates. A negative control well containing only solvent was also ready to correct the results. After a 48-h incubation at 5 % CO_2 atmosphere, the assay was quenched by MTT reagent [3-(4,5-dimethylthiazol-2-yl)-2,5-diphenyl tetrazolium bromide] dissolved in SDS (sodium dodecyl sulfate). Optical density was scanned under a multimode reader at 570 nm (reference at 600 nm) using Presto Blue Cell Viability Reagent. IC_{50} values were calculated from the linear correlation of the corrected percentage live of cells (%) versus the tested concentration of compounds (µg/mL). Each assay was conducted twice, and their analysis results were reported as averaged IC_{50} values. A similar protocol was also performed for the cisplatin as the positive control.

Molecular docking

Molecular docking was carried out using AutoDock Vina. The receptor (EGFR (3POZ) is downloaded from the protein data bank website (https://www.rcsb.org/). Water and cofactors are removed. Hydrogens are added to the receptor coordinates. Charges are added, all nonpolar hydrogens are merged, atom types are assigned using AutoDock Tools, and a .pdbqt file is generated. The binding site of the ligand and exhaustiveness parameter was determined as a Vina configuration file (see Supplementary material) [21]. Ligands were drawn using the Ketcher structure editor and saved as an sdf file. The 3D structure of the ligand was minimized using Avogadro with MMFF94. The sdf file was then further converted into a .pdbqt file using OpenBabel. Docking visualization and analysis were examined using UCSF ChimeraX and Biovia Discovery Studio Visualizer.

Results and discussion

Synthesis of 2-nitrocinnamaldehyde derivatives

The 2-Nitrocinnamaldehyde derivatives (**9** - **12**) were successfully synthesized through the Claisen-Schmidt condensation between the corresponding substituted aromatic acyl with *trans*-2-nitrocinnamaldehyde over basic condition (Scheme 1). Some modifications of the cited procedures were applied to obtain reasonable results. For instance, potassium hydroxide in the methanolic-water system was appropriately used to synthesize **10** - **11** and **12**. On the other hand, concentrated ethanolic sodium hydroxide was required to synthesize **9**. It is implied that the stronger the donating effect of the substituent, as shown in the order of **12**, **11**, **10**, and **9**, the weaker the acidity of the α-carbon of the acyl moiety. Thus, more bases were required to produce the related enolate intermediate [22] from the corresponding aromatic acyl derivatives. Alternatively, such acidic conditions may compromise the strength of the donating moiety toward the low acidity of the α-carbon of the acyl group through an enol intermediate formation [22].

Instead of base concentration, such an elevated temperature reaction was also necessary [23,24], particularly for the formation of **10** and **11** up to 50 °C, to speed up the dehydration step, leading to a reasonable chemical yield of the product. Such a nucleophile substitution at the a-carbon usually would normalize the reaction to mild conditions. However, a similar condition did not work for the formation of **9**, which produced a complex mixture containing the target product, byproducts, and the remaining precursors. More optimization of the key variables, such as using an alternative catalyst, employing an aprotic solvent, or Dean-Stark apparatus in toluene for facile water removal [10], must be explored. The aforementioned phenomena were supported relatively by the obtained chemical yield ranging from 29 - 99 %, which agreed with the yield of typical analog derivatives reported elsewhere [18,23,24].

Overall, the condensation in a basic medium (NaOH or KOH) is the most often used synthetic method for chalcone derivatives, even though the typical precursor substituents of the matching aldehyde and acetophenone have a substantial impact on the reaction time and byproducts [25]. In some cases, microwave irradiation has replaced conventional heating to increase the chemical yield of the products [9,26,27].

Spectroscopic analyses like UV/Vis FTIR, ^{1}H- and ^{13}C-NMR, and mass spectra were recorded and compared to the available literature to elucidate the target molecules' structure. A typical UV/Vis conjugated band of the unsaturated α, β-ketone **9**, **10**, **11**, and **12** was observed at 376, 323, 316, and 325 nm (SM **Figure A**), which was further confirmed by the FTIR spectra at the wavenumber of 1729, 1663, 1735, and 1662 cm^{-1} respectively (SM **Figure B**). In addition, the FTIR also revealed the presence of moieties of aromatic C-H at 3034-3105 cm^{-1}, C=C at 1606-1654 cm^{-1}, and C-NO_2 at 1514-1543 cm^{-1}. In particular, the group of -NH_2 of **9** was also found at 3341 cm^{-1}.

The ^{1}H-NMR analysis of **9** in DMSO-d_6 (SM **Figure 1(C)**) revealed the presence of 14 proton integrations consisting of 8 aromatic protons at 8.00 - 7.58 ppm, and 6.61 ppm, 4 methine protons at 7.25 - 7.44 ppm, and 2 amine protons at 6.18 ppm. However, the specific coupling constant of typical *trans*-conjugated alkene was not resolved distinctively. To support the ^{1}H-NMR data, the spectra of ^{13}C-NMR in a similar deuterated solvent (SM **Figure 1(D)**) assigned 17 carbon signals belonging to 1 carbonyl carbon at 186 ppm, 12 aromatic carbons at 154 - 113 ppm and 4 conjugated alkene carbons at 141 - 128 nm. Finally,

ToF-HRMS-ES$^+$ (SM **Figure 1(E)**) found the mass **9** as 295.1084 with a molecular formula of $C_{17}H_{14}N_2O_3$.

To confirm the structure of **10**, ^{1}H-NMR spectra in $CDCl_3$ (SM **Figure 2(C)**) identified the appearance of 12 protons composed of 8 aromatic protons at 8.00 - 7.56 ppm, 4 methine protons at 7.53 - 6.96 ppm. In addition to the ^{1}H-NMR data, a ^{13}C-NMR of **10** in a similar deuterated solvent (SM **Figure 2(D)**) confirmed the signal of 17 carbons. A chemical shift at 189 ppm was assigned to 1 carbonyl carbon, while at 148 - 124 ppm was identified as 12 carbons of aromatic benzene. Additionally, 4 conjugated alkene carbons were observed at 144 - 127 ppm. Lastly, the ToF-HRMS-ES$^+$ (SM **Figure 2(E)**) measured the mass of **10** as 358.0104 with a molecular formula of $C_{17}H_{12}BrNO_3$.

Comparatively, the ^{1}H-NMR of **11** in $CDCl_3$ (SM **Figure 3(C)**) also assigned 15 proton signals representing 8 aromatic protons at 7.99 - 7.30 ppm, 4 methine protons at 7.48 - 6.97 ppm, and 3 methyl protons at 2.43 ppm. As the complementary of the ^{1}H-NMR, the ^{13}C-NMR in the same solvent (SM **Figure 3(D)**) discovered 18 carbon signals, which were identified as 1 carbonyl carbon at 190 ppm, 12 carbons of aromatic benzene at 159 - 125 ppm, 4 conjugated alkene carbons at 143 - 128 ppm, and 1 methyl carbon at 21.83 ppm. Additional data of ToF-HRMS-ES$^+$ (SM **Figure 3(E)**) eventually confirmed the mass **11** as 294.1193 with a molecular formula of $C_{18}H_{15}NO_3$.

Following a similar pattern, the typical ^{1}H-NMR and ^{13}C-NMR spectra of **12** in $CDCl_3$ (SM **Figures 4(C)** and **4(D)**) also agreed with other derivatives. Twelve protons were detected on ^{1}H-NMR, representing 8 protons of aromatic benzene at 9.17 - 7.56 ppm and 4 methine protons at 7.56 - 6.99 ppm. In addition, the ^{13}C-NMR also verified a total of 16 carbons, consisting of 1 carbonyl carbon at 189 ppm, 11 carbons of aromatic benzene at 153 - 124 ppm, and 4 carbons of conjugated alkene at 145 - 127 ppm. Upon ToF-HRMS-ES$^+$ measurement (SM **Figure 4(E)**), a mass **12** was found 281.0924 with a molecular formula of $C_{16}H_{12}N_2O_3$. In general, the coupling constant of most derivatives resolved the *trans* geometry at 15 Hz, which was in agreement with the related standard constant [28]. Overall, the recorded signals aligned with the similar compounds of **10** and **11** reported previously [29,30] and with the analogs published elsewhere [29] for the new compounds of **9** and **12**.

Cytotoxicity assay on MCF-7 cells

The MTT assay of all derivatives against MCF-7 breast cancer lines was presented in **Table 1** as the IC_{50} of inhibition toward the viability of the cancer cells (SM: **Table F**, **Figures G,** and **H**). According to the cytotoxicity potency level reported by Prayong *et al.* [31], compound **12** exhibited relatively moderate inhibition against the cancer cell lines. On the other hand, the remaining compounds (**9**, **10**, and **11**) were classified as weak anti-cancer agents or not toxic. The methyl moiety installed in a benzene ring generally resulted in a poor antiproliferative, as Liew *et al.* [32] reported. Therefore, the derivative **11** might be an unfavorable substituent against anticancer activity. Regarding reactivity, the methyl moiety affected the molecule's center through the weakest positive inductive effect compared to others. In contrast, the *para*-amine and *para*-bromide exhibited more of a donating mesomeric effect. However, the pyridine moiety tended to show more electron-withdrawing impact than others.

As the MTT assay was performed in an aqueous system, the less soluble chalcone derivatives in the buffer might lower their toxicity. Such polar substituents installed in the related precursors of aldehyde or acetophenone plausibly increase the effective soluble concentration of the compound and exhibit more potent cytotoxicity [25].

Table 1 Cytotoxic assay of *o*-Nitrocinnamaldehyde derivatives against MCF-7 cancer cells.

Sample	IC_{50} (µg/mL)
Compound **9**	178
Compound **10**	376
Compound **11**	>500
Compound **12**	118

Based on the chemical reactivity and bioactivity relationship, it was implied that typical electron-withdrawing substituent at the acetophenone side demonstrated more potent cytotoxicity against MCF-7. Such SAR evidence was reported that most electron-withdrawing groups at the appropriate position played an essential role in anticancer activity instead of α, β-unsaturated carbonyl [32]. In particular, a conformational restrain was reported to decrease the cytotoxic activity of typical chalcone derivatives [33]. An inhibition of aromatase targeting CyP19A1 was well-known as the cytotoxic activity mechanism of an active compound against MCF-7 cell lines [34]. Further molecular docking of a typical polycyclic skeleton with the targeted aromatase [35] revealed that an olefinic moiety provided a protein-binding nature towards the bioactive compounds, while an electron-withdrawing group such as carboxylic acid was responsible for the MCF-7 inhibition. However, further molecular docking must be performed to understand how effectively the derivatives interacted with the MCF-7 receptor. Thus, a better structural design can be obtained before the laboratory synthesis.

Molecular docking study

MCF-7 cancer cell lines' proliferation correlates with estrogen receptor alpha (ERα) regulation. The proliferation of MCF-7 was promoted through ERα suppressing the p53/p21 signal and up-regulating proliferating cell nuclear antigen (PCNA) and Ki-67 antigen [36]. Tamoxifen is an antagonist in human breast cancer and is classified as a selective estrogen receptor modulator (SERM) [37]. Several clinical studies showed that acquired tamoxifen resistance in MCF-7 correlates with increased EGFR/HER2 expression. The combination treatment with EGFR inhibitors such as Gefitinib showed tamoxifen response improvement and delayed acquired resistance in the MCF-7 cancer cell line [38]. Gefitinib inhibits the phosphorylation of EGFR by competitively binding with ATP into the kinase domain (KD) of EGFR. Hence, in this paper, the interaction of compounds **9** and **12** with EGFR was studied by the molecular docking method [39].

This molecular docking study used the co-crystal structure EGFR (PDB ID: 3POZ [40], and dual EGFR/HER2 inhibitor TAK-285 [41]. The docking configuration was validated by obtaining an RMSD value of 1.3 Å from reduced TAK-285 into the kinase domain of 3POZ. In our model (**Figure 2**), the nitrogen of TAK-285's pyrimidine ring formed a hydrogen bond with Met793 of the hinge region, and the trifluoromethyl moiety formed H-bonds with Thr854, Thr790, and Leu777 and made several other interactions with Met766, Phe856, Cys775, Arg776, and Leu788. The chloro-aniline moiety made H-bonds with Thr854 and several noncovalent interactions with Lys745, Ala743, and Val726, while N-ethyl-3-hydroxy-3-methylbutanamide was oriented towards the solvent region and made Van der Waals interactions with Arg841, Gly796, Gly719, and Asn842. The binding energy obtained from interactions was 10.692 kcal/mol.

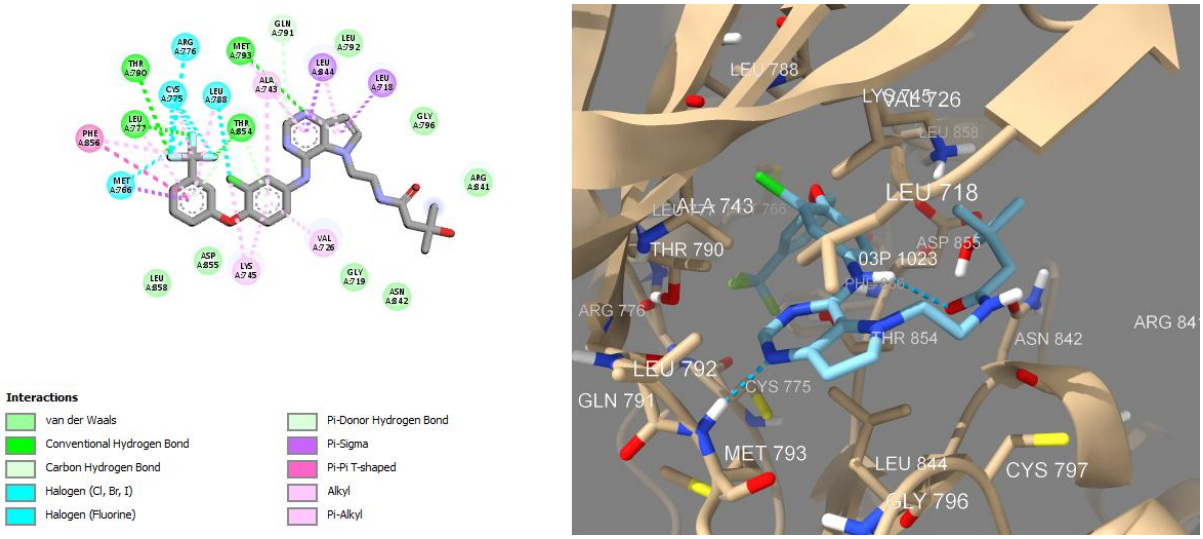

Figure 2 2D and 3D interaction of TAK-285 with EGFR (3POZ) (In the 3D model, H-bonds: Dashed blue color).

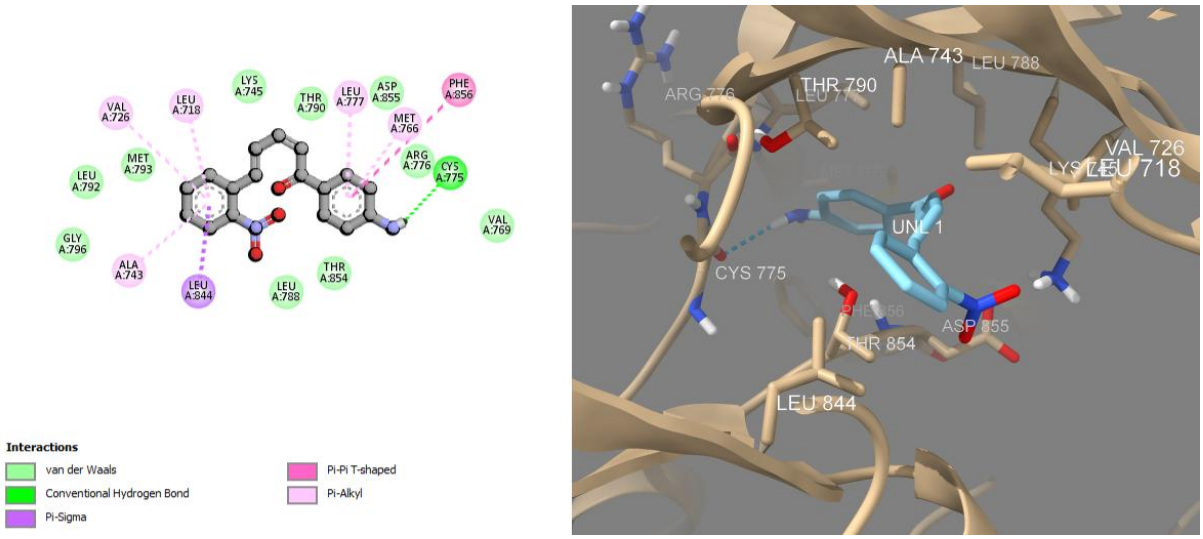

Figure 3 2D and 3D interaction of compound **9** with EGFR (3POZ) (In the 3D model, H-bonds: Dashed blue color).

Instead of the hydrogen bonding formation with Met793, the nitrophenyl moiety of compound **9** formed a Van der Waals interaction (**Figure 3**). In this region, nitrophenyl was sandwiched between Leu844 and Leu718. The phenacyl moiety of compound **9** contributed a hydrogen bond with Cys775 and made several noncovalent interactions with Met766, Leu777, and Phe856. The binding energy of compound **9** was –8.506 kcal/mol. The nitrophenyl moiety of compound **12** adopts a different conformation with compound **9**; the nitro functional groups move closer and make H-bond to Met793 residue. Nitrophenyl also made noncovalent interactions with Leu718 and Val726. The acetyl pyridine of compound **12** formed an H-bond with Lys745 and Thr854, and its ring formed a Pi-alkyl noncovalent interaction with Leu788 residue (**Figure 4**). Compound 12's binding energy (–8.555 kcal/mol) was slightly lower than compound **9**.

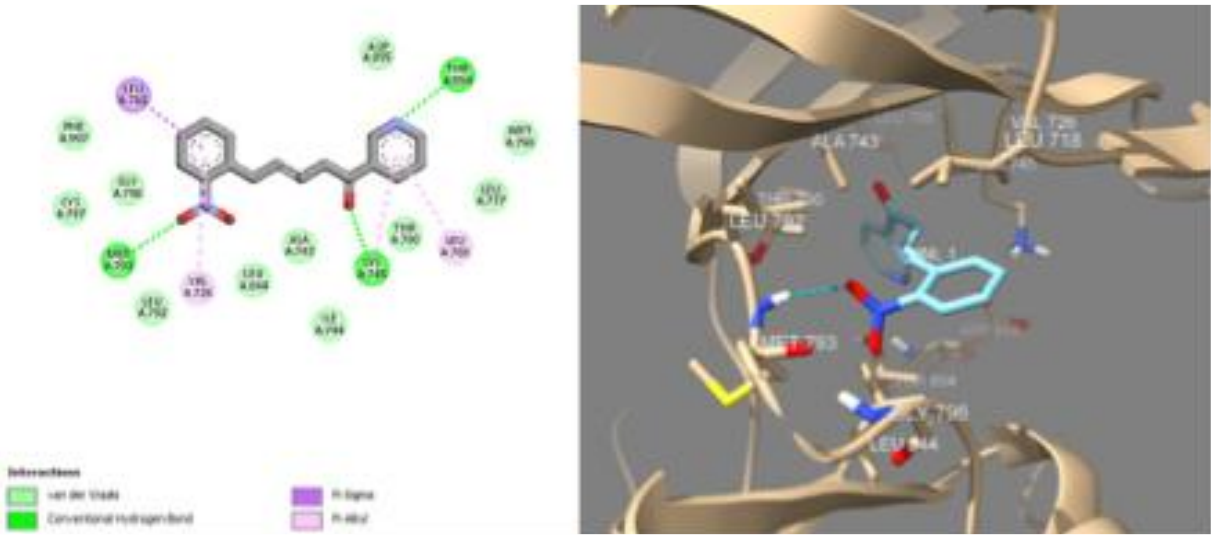

Figure 4 2D and 3D interaction of compound **12** with EGFR (3POZ) (In the 3D model, H-bonds: Dashed blue color).

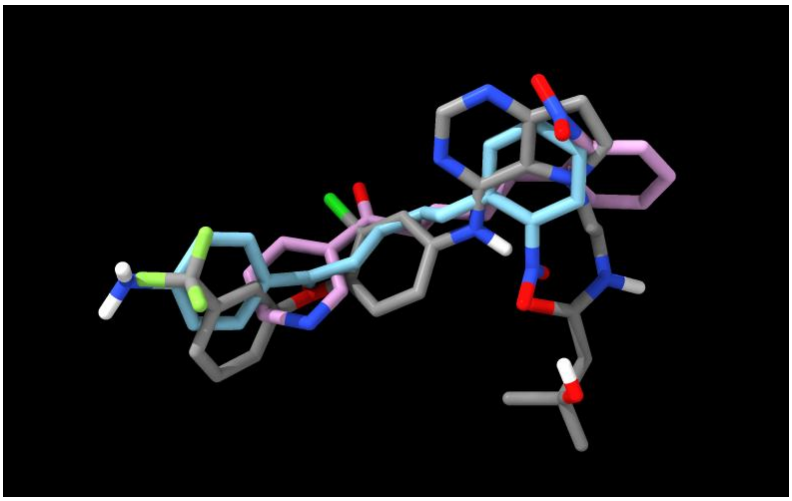

Figure 5 Superimposed structure of TAK-285 (grey), compound **9** (blue), and compound **12** (pink).

The superimposed structure showed that TAK-285 has one fused heterocyclic ring and 2 aromatic rings, each linked with amino and ether linker (**Figure 5**). Fused heterocyclics are commonly found features in the EGFR kinase inhibitors. They mimic the adenine of ATP, so their nitrogen can form hydrogen bonding with the hinge region of the kinase domain of EGFR. The heterocyclic ring is linked with the aryl ring through an amino linker to occupy the back pocket of EGFR. To enhance activity towards EGFR, an aryl ring is further added through an ether linker in the inhibitor's skeleton, resulting in dual inhibitory activity towards EGFR and HER2. In addition, a long alkyl chain of inhibitor is used to interact with the solvent region of the receptor (**Figure 6(a)**) [42].

Compounds **9** and **12** need several structural features compared to known kinase inhibitors (**Figures 5** and **6(b)**). Further structural modification to **9** and **12** is necessary to improve their biological activity. Hypothetically, both compounds can undergo intermolecular Michael addition to form a fused heterocyclic ring resembling a quinazoline/quinoline core [43]. Another example is using hydrazine or hydroxylamine to introduce heterocyclic rings into **9** and **12** (**Figure 6(b)**) [44,45]. Such moieties enhanced potent cytotoxicity against cancer cells or other pharmacological activities [9,46-49]. The proposed structural modification (compound **13**) was docked into the EGFR catalytic domain (**Figure 7**). The heterocyclic moiety of compound **13** occupied the hinge region and created several interactions with Met793, Leu792, and Ala743. The acetophenone moiety occupied the hydrophobic region and formed pi-pi interaction notably with Phe856, and their chlorine and fluorine atoms

created interactions with Met766, Cys775, and Arg776. These key residues influenced the binding affinity between the inhibitor and EGFR [38]. At the same time, compound **13**'s propylmorpholine extended into the accessible area. These are 3 essential pharmacophores commonly found in small-molecule EGFR kinase inhibitors. We expect to validate the anticancer capability of compound **13** with further *in-vitro* assays shortly.

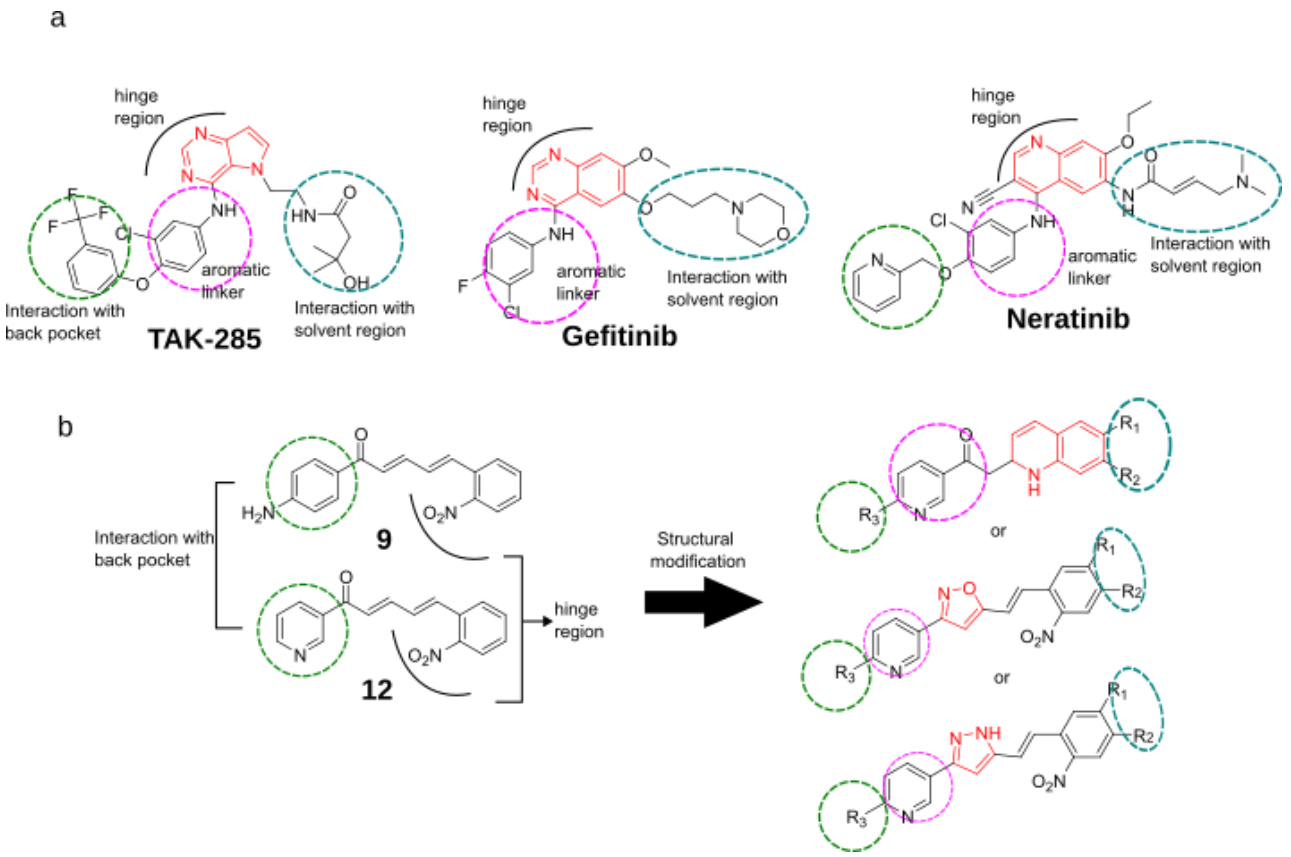

Figure 6 Common structural features of EGFR/HER2 inhibitors (a) and further structural modification of **9** and **12** (b).

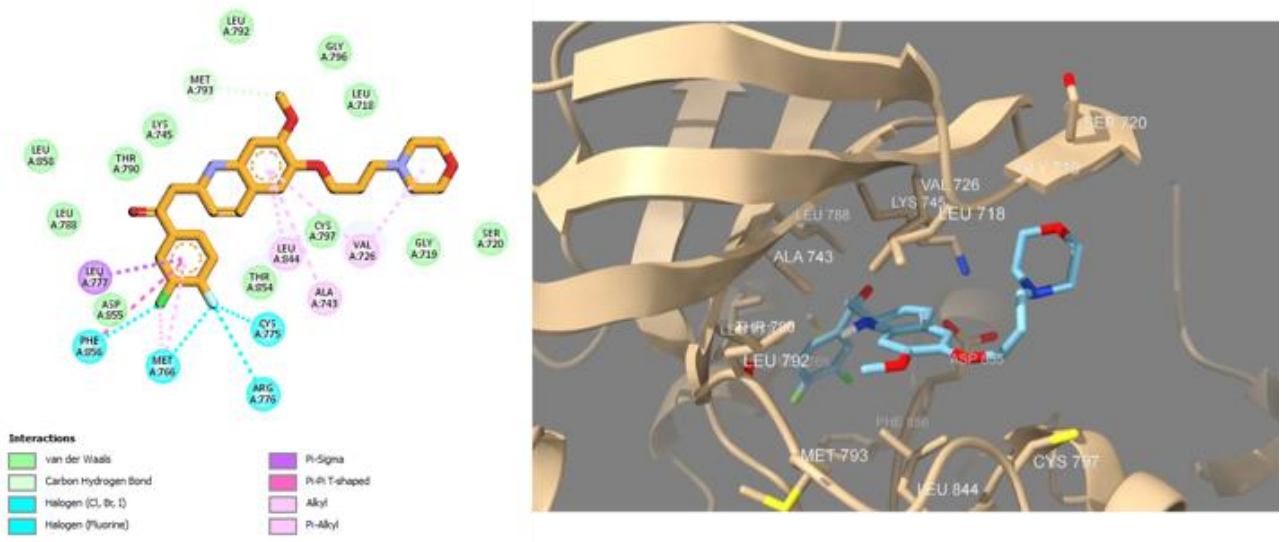

Figure 7 2D and 3D interaction of compound **13** with EGFR (3POZ).

Conclusions

In one-pot Schmidt-Claisen condensation, 4 compounds of *o*-Nitrocinnamaldehyde-based derivatives (**9** - **12**) were effectively synthesized with a chemical yield of 29 - 99 %. Compound **12** was the most potential derivative as anti-cancer MCF-7 (IC_{50} of 118 µg/mL), among others. Based on a bioinformatics investigation, additional skillful structural modification of **12** frameworks may raise its moderate toxicity to a more potent level. Thereby, it may be utilized further as an anticancer agent.

Acknowledgements

The research funding was supported by KemenDikBud-Ristek (PFR-No.3919/UN6.3.1/PT.00/2024) and Laboratory of Natural Product Bioactive Compound, Universitas Jambi 2022. We thank Laboratorium Kimia Terpadu FMIPA-ITB for the NMR analysis and Central Laboratory of Universitas Padjadjaran for the Bioassay

References

[1] J Ferlay, HR Shin, F Bray, D Forman, C Mathers and DM Parkin. Estimates of worldwide burden of cancer in 2008: GLOBOCAN 2008. *International Journal of Cancer* 2010; **127**, 2893-2917.

[2] B Costa, I Amorim, F Gärtner and N Vale. Understanding Breast cancer: From conventional therapies to repurposed drugs. *European Journal of Pharmaceutical Sciences* 2020; **151**, 105401.

[3] V Schirrmacher. From chemotherapy to biological therapy: A review of novel concepts to reduce the side effects of systemic cancer treatment (Review). *International Journal of Oncology* 2019; **54(2)**, 407-419.

[4] S Haryanti and Y Widiyastuti. Cytotoxic activity of Indonesian plants on MCF-7 cell lines for traditional breast cancer treatment (*in Indonesian*). *Media Penelitian dan Pengembangan Kesehatan* 2017; **27(4)**, 247-254.

[5] EB Elkaeed, HAAE Salam, A Sabt, GH Al-Ansary and WM Eldehna. Recent advancements in the development of anti-breast cancer synthetic small molecules. *Molecules* 2021; **26(24)**, 7611.

[6] M Naufal, E Hermawati, YM Syah, AT Hidayat, IW Hidayat and J Al-Anshori. Structure-activity relationship study and design strategies of hydantoin, thiazolidinedione, and rhodanine-based kinase inhibitors: A two-decade review. *ACS Omega* 2024; **9**, 4186-4209.

[7] R Leechaisit, P Mahalapbutr, P Boonsri, K Karnchanapandh, T Rungrotmongkol, V Prachayasittikul, S Prachayasittikul, S Ruchirawat, V Prachayasittikul and R Pingaew. Discovery of novel naphthoquinone-chalcone hybrids as potent FGFR1 tyrosine kinase inhibitors: Synthesis, biological evaluation, and molecular modeling. *ACS Omega* 2023; **8(36)**, 32593-32605.

[8] L Wang, W Fan, L Cui, N Yang, X Zhang, S Yu, Y Li and B Wang. Synthesis and biological activity evaluation of novel chalcone analogues containing a methylxanthine moiety and their N-acyl pyrazoline derivatives. *Journal of Agricultural and Food Chemistry* 2023; **71(49)**, 19343-19356.

[9] K Mezgebe, Y Melaku and E Mulugeta. Synthesis and pharmacological activities of chalcone and its derivatives bearing n-heterocyclic scaffolds: A review. *ACS Omega* 2023; **8(22)**, 19194-19211.

[10] C Zhuang, W Zhang, C Sheng, W Zhang, C Xing and Z Miao. Chalcone: A privileged structure in medicinal chemistry. *Chemical Reviews* 2017; **117**, 7762-7810.

[11] NAA Elkanzi, H Hrichi, RA Alolayan, W Derafa, FM Zahou and RB Bakr. Synthesis of chalcones derivatives and their biological activities: A review. *ACS Omega* 2022; **7(32)**, 27769-27786.

[12] GD Yadav and DP Wagh. Claisen-Schmidt condensation using green catalytic processes: A critical review. *ChemistrySelect* 2020; **5(29)**, 9059-9085.

[13] CB Patil, SK Mahajan and SA Katti. Chalcone: A versatile molecule. *Journal of Pharmaceutical Sciences and Research* 2009; **1(3)**, 11-22.

[14] G Wang, W Liu, Z Gong, Y Huang, Y Li and Z Peng. Synthesis, biological evaluation, and molecular modelling of new naphthalene-chalcone derivatives as potential anticancer agents on MCF-7 breast cancer cells by targeting tubulin colchicine binding site. *Journal of Enzyme*

Inhibition and Medical Chemistry 2020; **35**, 139-144.

[15] S Syam, SI Abdelwahab, MA Al-Mamary and S Mohan. Synthesis of chalcones with anticancer activities. *Molecules* 2012; **17(6)**, 6179-6195.

[16] CW Mai, M Yaeghoobi, N Abd-Rahman, YB Kang and MR Pichika. Chalcones with electron-withdrawing and electron-donating substituents: Anticancer activity against TRAIL resistant cancer cells, structure-activity relationship analysis and regulation of apoptotic proteins. *European Journal of Medical Chemistry* 2014; **77**, 378-387.

[17] HO Saxena, U Faridi, JK Kumar, S Luqman, MP Darokar, K Shanker, CS Chanotiys, MM Gupta and AS Negi. Synthesis of chalcone derivatives on steroidal framework and their anticancer activities. *Steroids* 2007; **72(13)**, 892-900.

[18] DJ Weldon, MD Saulsbury, J Goh, L Rowland, P Campbell, L Robinson, C Miller, J Christian, L Amis, N Taylor, C Dill, WJ Davis, SL Evans and E Brantley. One-pot synthesis of cinnamylideneacetophenones and their *in vitro* cytotoxicity in breast cancer cells. *Bioorganic & Medicinal Chemistry Letters* 2014; **24(15)**, 3381-3384.

[19] A Zainuddin, SR Meilanie, Darwati, Kurniawan, Nurlelasari, T Herlina, AR Saputra, JA Anshori and T Mayanti. Cytotoxic triterpenoids from the stem barks of *Dysoxylum arborescens* and *Dysoxylum excelsum* against MCF-7 breast cancer cell. *Sains Malaysiana* 2020; **49(5)**, 989-994.

[20] T Mayanti, SA Azahra, TP Syafriadi, N Nurlelasari, R Maharani, E Julaeha, U Supratman, SE Sinaga, S Ekawardhani and S Fajriah. Onoceranoid triterpenes of *Lansium domesticum* Corr. cv. Kokossan and their cytotoxicity against MCF-7 breast cancer cells. *Trends in Sciences* 2024; **22(1)**, 9000.

[21] S Forli, R Huey, ME Pique, MF Sanner, DS Goodsell and AJ Olson. Computational protein-ligand docking and virtual drug screening with the AutoDock suite. *Nature Protocols* 2016; **11(5)**, 905-919.

[22] AT Nielsen and WJ Houlihan. *The aldol condensation*. Wiley, New Jersey, 2011.

[23] YS Kil, SK Choi, YS Lee, M Jafari and EK Seo. Chalcones from Angelica keiskei: Evaluation of their heat shock protein inducing activities. *Journal of Natural Products* 2015; **78**, 2481-2487.

[24] Y Ren, C Yuan, Y Qian, HB Chai, X Chen, M Goetz and AD Kinghorn. Constituents of an extract of *Cryptocarya rubra* housed in a repository with cytotoxic and glucose transport inhibitory effects. *Journal of Natural Products* 2014; **77(3)**, 550-556.

[25] SL Gaonkar and UN Vignesh. Synthesis and pharmacological properties of chalcones: A review. *Research on Chemical Intermediates* 2017; **43(11)**, 6043-6077.

[26] P Kulkarni. Calcium oxide catalyzed synthesis of chalcone under microwave condition. *Current Microwave Chemistry* 2015; **2(2)**, 144-149.

[27] D Rocchi, JF González and JC Menéndez. Montmorillonite clay-promoted, solvent-free cross-aldol condensations under focused microwave irradiation. *Molecules* 2014; **19(6)**, 7317-7326.

[28] T Liptaj, M Remko and J Polčin. Analysis of 1H-NMR spectra of cinnamaldehyde type model substances of lignin. *Collection of Czechoslovak Chemical Communications* 1980; **45**, 330-334.

[29] CR Polaquini, GS Torrezan, VR Santos, AC Nazaré, DL Campos, LA Almeida, IC Silva, H Ferreira, FR Pavan, C Duque and LO Regasini. Antibacterial and antitubercular activities of cinnamylideneacetophenones. *Molecules* 2017; **22(10)**, 1685.

[30] H Zhang, H Jin, L Ji, K Tao, W Liu, HY Zhao and TP Hou. Design, synthesis, and bioactivities screening of a diaryl ketone-inspired pesticide molecular library as derived from natural products. *Chemical Biology & Drug Design* 2011; **78(1)**, 94-100.

[31] P Prayong, S Barusrux and N Weerapreeyakul. Cytotoxic activity screening of some indigenous Thai plants. *Fitoterapia* 2008; **79(7-8)**, 598-601.

[32] SK Liew, S Malagobadan, NM Arshad and NH Nagoor. A review of the structure-activity relationship of natural and synthetic antimetastatic compounds. *Biomolecules* 2020; **10(1)**, 138.

[33] ML Go, X Wu and XL Liu. Chalcones: An update on cytotoxic and chemoprotective properties. *Current Medical Chemistry* 2005; **12(4)**, 483-499.

[34] Y Shibahara, Y Miki, Y Onodera, S Hata, MSM Chan, CC Yiu, TY Loo, Y Nakamura, JI Akahira, T Ishida, K Abe, H Hirakawa, LW Chow, T Suzuki, N Ouchi and H Sasano. Aromatase inhibitor treatment of breast cancer cells increases the expression of let-7f, a microRNA targeting CYP19A1. *Journal of Pathology* 2012; **227(3)**, 357-366.

[35] O Prakash, A Ahmad, VK Tripathi, S Tandon, AB Pant and F Khan. *In silico* assay development for screening of tetracyclic triterpenoids as anticancer agents against human breast cancer cell line MCF7. *PLoS One* 2014; **9(11)**, e111049.

[36] XH Liao, DL Lu, N Wang, LY Liu, Y Wang, YQ Li, TB Yan, XG Sun, P Hu and TC Zhang. Estrogen receptor α mediates proliferation of breast cancer MCF-7 cells via a p21/PCNA/E2F1-dependent pathway. *FEBS Journal* 2014; **281**, 927-942.

[37] AK Shiau, D Barstad, PM Loria, L Cheng, PJ Kushner, DA Agard and GL Greene. The structural basis of estrogen receptor/coactivator recognition and the antagonism of this interaction by tamoxifen. *Cell* 1998; **95(7)**, 927-937.

[38] S Massarweh, CK Osborne, CJ Creighton, L Qin, A Tsimelzon, S Huang, H Weiss, M Rimawi and R Schiff. Tamoxifen resistance in breast tumors is driven by growth factor receptor signaling with repression of classic estrogen receptor genomic function. *Cancer Research* 2008; **68(3)**, 826-833.

[39] CH Yun, TJ Boggon, Y Li, MS Woo, H Greulich, M Meyerson and MJ Eck. Structures of lung cancer-derived EGFR mutants and inhibitor complexes: Mechanism of activation and insights into differential inhibitor sensitivity. *Cancer Cell* 2007; **11(3)**, 217-227.

[40] K Aertgeerts, R Skene, J Yano, BC Sang, H Zou, G Snell, A Jennings, K Iwamoto, N Habuka, A Hirokawa, T Ishikawa, T Tanaka, H Miki, Y Ohta and S Sogabe. Structural analysis of the mechanism of inhibition and allosteric activation of the kinase domain of HER2 protein. *Journal of Biological Chemistry* 2011; **286(21)**, 18756-18765.

[41] T Doi, H Takiuchi, A Ohtsu, N Fuse, M Goto, M Yoshida, N Dote, Y Kuze, F Jinno, M Fujimoto, T Takubo, N Nakayama and R Tsutsumi. Phase I first-in-human study of TAK-285, a novel investigational dual HER2/EGFR inhibitor, in cancer patients. *British Journal of Cancer* 2012; **106(4)**, 666-672.

[42] T Ishikawa, M Seto, H Banno, Y Kawakita, M Oorui, T Taniguchi, Y Ohta, T Tamura, A Nakayama, H Miki, H Kamiguchi, T Tanaka, N Habuka, S Sogabe, J Yano, K Aertgeerts and K Kamiyama. Design and synthesis of novel human epidermal growth factor receptor 2 (HER2)/epidermal growth factor receptor (EGFR) dual inhibitors bearing a pyrrolo[3,2-d]pyrimidine scaffold. *Journal of Medicinal Chemistry* 2011; **54(23)**, 8030-8050.

[43] AL Tökés, GY Litkei and L Szilágyi. N-heterocycles by cyclization of 2′-Nhr-Chalcones, 2′-Nhr-Chalcone dibromides and 2′-Nhr-α-Azidochalcones. *Synthetic Communications* 1992; **22**, 2433-2445.

[44] M El-Naggar, HRM Rashdan and AH Abdelmonsef. Cyclization of chalcone derivatives: Design, synthesis, *in silico* docking study, and biological evaluation of new quinazolin-2,4-diones incorporating five-, six-, and seven-membered ring moieties as potent antibacterial inhibitors. *ACS Omega* 2023; **8(30)**, 27216-27230.

[45] A Voskienė and V Mickevičius. Cyclization of chalcones to isoxazole and pyrazole derivatives. *Chemistry of Heterocyclic Compounds* 2009; **45**, 1485-1488.

[46] S El-Kalyoubi, SA El-Sebaey, AA El-Sayed, MS Abdelhamid, F Agili and SM Elfeky. Novel pyrimidine Schiff bases and their selenium-containing nanoparticles as dual inhibitors of CDK1 and tubulin polymerase: Design, synthesis, anti-proliferative evaluation, and molecular modelling. *Journal of Enzyme Inhibition and Medical Chemistry* 2023; **38(1)**, 2232125.

[47] S El-Kalyoubi, MM Khalifa, MT Abo-Elfadl, AA El-Sayed, A Elkamhawy, K Lee and AA Al-Karmalawy. Design and synthesis of new spirooxindole candidates and their selenium nanoparticles as potential dual Topo I/II inhibitors,

DNA intercalators, and apoptotic inducers. *Journal of Enzyme Inhibition and Medical Chemistry* 2023; **38(1)**, 2242714.

[48] ZS Alshehri, FF Alshehri, SF Belasy, EA El-Hefny, MS Aly, AA El-Sayed and NA Hassan. Biochemical and preclinical evaluation with synthesis and docking study of pyridopyrimidines and selenium nanoparticle drugs for cancer targeting. *Current Nanoscience* 2025; **21(6)**, 498-510.

[49] LO El-Halaby, NFA El-Magd, SJ Almehmadi, AA El-Sayed, RR Khattab, S El-Kalyoubi and SM Elfeky. Synthesis, *In-Vitro*, *In-Vivo* screening, and molecular docking of disubstituted aminothiazole derivatives and their selenium nanoparticles as potential antiparkinson agents. *Journal of Molecular Structure* 2024; **1315**, 138951.